PROGRESS
IN COLOR, COLORANTS AND COATINGS

available online @ www.pccc.icrc.ac.ir
Prog. Color Colorants Coat. 2(2009), 35-43

Ministry of Science, Research and Technology
Institute for Color Science and Technology

Synthesis and Characterization of Nanocrystalline Magnetic Pigment via Coordinated Precursors

M. Gharagozlou
Assistant Professor, Department of Nanotechnology and Nanomaterials, Institute for Color Science and Technology, P.O.Box: 16765-654, Tehran, Iran

ARTICLE INFO

Article history:
Received: 20-9-2008
Accepted: 23-12-2008
Available online: 12-3-2009

Keywords:
Magnetic pigments
Nanocrystalline
Cobalt ferrite
Coordinated precursors
Chemical synthesis.

ABSTRACT

Nanocrystalline cobalt ferrite as a magnetic black pigment was synthesized via coordinated precursors with a significant decrease of the synthesis temperature using citric acid as a coordinating agent. The structure and properties of the cobalt ferrite powder were characterized by X-ray diffraction (XRD), colorimetric analysis ($L^*a^*b^*$ color parameters), diffuse reflectance spectroscopy and vibrating sample magnetometer (VSM). In addition, the structural coordination and morphology of the precursors and cobalt ferrite powder were evaluated by infrared spectroscopy (FTIR) and scanning electron microscopy (SEM). Simultaneous thermal analysis (TG-DTG-DTA) was used to investigate the thermal decomposition of the coordinated precursor. FTIR spectra of the precursors indicated that carboxylate groups of citric acid coordinated to the metal ions to form the coordinated precursors. Diffraction patterns and FTIR spectrum confirmed the formation of a pure organic free single-phase spinel with a cubic system (Fd3m). The crystallite size was in the range of 18-22 nm using Scherrer equation. The SEM micrographs showed changes in the morphology of the precursors and in the sample in which the cobalt ferrite powder had almost spherical morphology. Colorimetric analysis using $L^*a^*b^*$ coordinates and diffuse reflectance spectroscopy revealed nearly full light absorption in the 350-750 nm range which are in agreement with the black color of the cobalt ferrite pigment. Values of the saturation magnetization (M_s), remanent magnetization (M_r) and magnetic coercivity (H_c) corresponding to the cobalt ferrite powder were: 67.72 emu/g, 32.54 emu/g and 1.8 kOe, respectively. They were lower than the bulk values because of the nanoscale of the powder. Prog. Color Colorants Coat. 2(2009), 35-43. © Institute for Color Science and Technology.

1. Introduction

Magnetic pigments have been intensively studied because of their applicability in a variety of areas such as high-density information storage, magnetizable printing ink, ferrofluid technology, magnetic drug delivery, magnetocaloric refrigeration, medical diagnostic, catalyst, magnetic resonance imaging enhancement and gas sensing [1-6]. Amongst spinel ferrites, cobalt ferrite

---

*Corresponding author: gharagozlou@icrc.ac.ir has attracted considerable attention due to the high magnetocrystalline anisotropy, high coercivity, moderate saturation magnetization, large magnetostrictive coefficient, chemical stability and mechanical hardness.

the spinel, with general formula 'AB_2O_4'(A refers to cations in tetrahedral sites, and B refers to cations in the octahedral positions), is a cubic structure with space group of symmetry Fd3m. This elaborate crystallographic structure, which can accommodate significant cations in the disordered form, has a unique perspective for studies of substitutions and their relations with the chemical and physical properties [2].

In the spinel crystallographic structures, two cation configurations are possible. The normal structure presents the $A(B_2)O_4$ distribution and the inverse one the $B(AB)O_4$. In both cases the parentheses indicate the octahedral sites.

Many works present the synthesis of spinel ferrites using a conventional ceramic powder preparation process, which involves a solid state reaction. This method has some disadvantages for advanced applications, such as: formation of strongly bonded agglomerates, non-homogeneities, such as: undesirable phases, abnormal grain growth, poor reproducibility and imprecise control of the cation stoichiometry and ratios [7].

In order to improve properties of the ferrite powders, chemical methods have been investigated recently [6]. These methods lead to a more precise stoichiometry and good sinterability, besides the particle size and morphology control [7]. In general, chemical techniques have some advantages over conventional ones in which the precursor presents high reactivity resulting in sintering temperature and/or time reduction [7].

The physical and chemical properties of spinel ferrites are greatly affected by the synthesis route. For this reason, various methods have been reported in literatures for preparation of these nanoscale spinel particles including coprecipitation [1], oxidation of the ferrous hydroxide gels using KNO_3 [8], oil-in-water emulsion route [9], hydro/solvothermal processes [10] and thermal decomposition of the different types of precursors such as $Fe(acac)_3$ and $Fe(CO)_5$ [11]. Although studies have been performed on the preparation of inorganic compounds using the coordinated precursors [12], there is rare information about the preparation of cobalt ferrite via coordinated precursors. This method has received a lot of attention due to its simplicity, low cost, homogeneous mixing at molecular level, good stoichiometric control, low processing temperature and the use of an aqueous based processing system. In earlier works we have synthesized and characterized several coordinated complexes [13-16].

Here, we report on the synthesis and characterization of nanocrystalline magnetic pigment via the coordinated precursor with a significant decrease of the calcined temperature using citric acid as a coordinating agent and ethylene glycol as an esterification agent.

2. Experimental

All the reagents were of the analytical grade (obtained from Merck) and used without further purification. Stoichiometric amounts (molar ratio of Co/Fe = 1:2) of $Fe(NO_3)_3.9H_2O$ and $Co(NO_3)_2.6H_2O$ aqueous solutions were mixed with the stoichiometric amounts of citric acid and ethylene glycol aqueous solutions. The molar ratio of the total metal ions to citric acid was kept as 1:3. The flask containing this mixture was then placed in a water bath and the temperature of the solution was raised to 65 °C. The viscosity of the solution was increased without any visible phase separation. The resulted gel (precursor I) was heat treated at 300 °C for 1 h (primary calcination), leading to the expansion to three times of its original volume and the formation of the porous semi-carbonized powder precursor (precursor II). The powder precursor was easily deagglomerated in a mortar and calcined on the alumina plate at 500 °C for 2 hours, with a heating rate of 10 °C/min in the ambient atmosphere.

FTIR spectra (500-4000 cm^{-1}) were recorded on a Perkin Elmer Spectrum One spectrophotometer with KBr pellets. Thermal analysis (TG-DTG-DTA) was carried out using a Perkin Elmer simultaneous thermal analyzer (STA Pyris Diamond Model) with the heating rate of 5 °C/min in flowing air. X-ray diffraction (XRD) was performed on a Philips PNA-analytical diffractometer using CuKα radiation (λ = 1.5406 A). SEM micrographs were obtained on a LEO 1455VP scanning electron microscope. Measurement of $L^*a^*b^*$ color parameters and diffuse reflectance spectrum of the cobalt ferrite pigment were carried out on a spectrophotometer CE-7000A, in the 350-750 nm range using the D65 illumination. Magnetic properties studied using Vibrating Sample Magnetometer (EG&G VSM Model 155) with a maximum applied field of 10 kOe at room temperature. From the obtained hysteresis loops, the saturation magnetization (M_s), remanent magnetization (M_r) and magnetic coercivity (H_c) were determined.

3. Results and discussion

Nanocrystalline magnetic black pigment, cobalt ferrite, was synthesized via coordinated precursors with a significant decrease of the synthesis temperature using citric acid as a coordinating agent. This method has been used as an alternative to the conventional sol-gel method to obtain nanocrystaline materials for different applications because of the low cost, versatility, control of the stoichiometry, its simplicity, low processing temperature, high degree of homogeneity since the reagents had been mixed at the molecular level.

The objective of this method was the immobilization of metallic ions in a rigid polymeric net. First, the chelates were formed between metal ions and citric acid. Later, ethylene glycol was added and heated to obtain a polymeric resin where the cations were uniformly distributed. This polymeric net was obtained from a solution containing ethylene glycol, citric acid and the respective cations. Heating of the polymeric resin caused a breakdown of the polymer. The following step was the calcination of breakdown polymer at known temperature for several hours to obtain the nanocrystalline material. Then, the coordination of metallic ions, the esterification and the polymerization reactions occured during the method, lead to the formation of the coordinated gel precursor [17].

Generally, presence of two functional groups in ethylene glycol leads to the polyesterification. It is important to emphasize that a better polymerization leads to the immobilization of cations in the polymeric net, and consequently, to a higher homogeneity of the final product, as this immobilization avoids the cation segregation.

Figure 1 shows the FTIR spectra of the precursors I. Infrared spectroscopy can be used to identify the resonant frequencies due to the rotation or vibration corresponding to discrete energy levels which are determined by the molecular potential energy levels and the masses of atoms.

The observed peaks at about 3400 and 1732 cm^{-1} are attributed to the stretching vibration of hydroxyl groups and uncoordinated carbonyl groups, respectively. The medium-weak bands at around 2990 and 3018cm^{-1} are assigned to the aliphatic and aromatic C-H bond stretching, respectively. An absorption band at 1074 cm^{-1} is due to the C-O bond stretch associated with the formation of the ester from the $-CH_2-OH$ group in ethylene glycol and the carboxylate group of citric acid [18].

In the FTIR spectra of the precursor I, the observed peaks observed at around 1601 and 1363 cm^{-1} are related to the asymmetric $\nu_{as}(COO)$ and symmetric $\nu_s(COO)$ stretching vibration of COO groups, respectively, which corroborate the coordination of metal ions by carboxylates groups to form a complex [18]. This gives rise to a large difference between $\nu_{as}(COO)$ and $\nu_s(COO)$, $\Delta\nu$ ($\nu_{as}(COO)-\nu_s(COO)$) about 238 cm^{-1}, the characteristic of the monodentate coordination of carboxylate groups to the metal ions [18] which confirms the presence of the coordinated precursor.

In the FTIR spectrum of the semi-carbonized precursor II (Figure 2) the absence of some of the organic bands could be ascribed to the decomposition of the most of the organic ligands in the gel after primary calcinations. However, the low intensity bands duo to the asymmetric $\nu_{as}(COO)$ and symmetric $\nu_s(COO)$ stretching vibration of the COO groups with $\Delta\nu$ ($\nu_{as}(COO)-\nu_s(COO)$) about 232 cm^{-1} , is the characteristic of the monodentate coordination of carboxylate groups to the metal ions [18] and confirms the presence of the coordinated precursor. In addition, the vibrating band at around 590 cm^{-1} corresponds to the metal-oxide ν(M-O) stretching vibration, and characteristic of the cobalt ferrite [18].

It can be seen that the FTIR spectrum of the cobalt ferrite powder (Figure 3) shows no residual organic compounds and confirms the formation of the organic free cobalt ferrite. The metal-oxide ν(M-O) stretching vibration at around 592 cm^{-1} is the characteristic of the cobalt ferrite. This peak may shift to higher wave numbers by substituting rare earth elements in the cobalt ferrite because of the distortion which happened in the tetrahedral and octahedral sites after doping [3]. Figure 4 shows the comparison between FTIR spectra of the precursor I (a), precursor II (b) and cobalt ferrite powder (c).

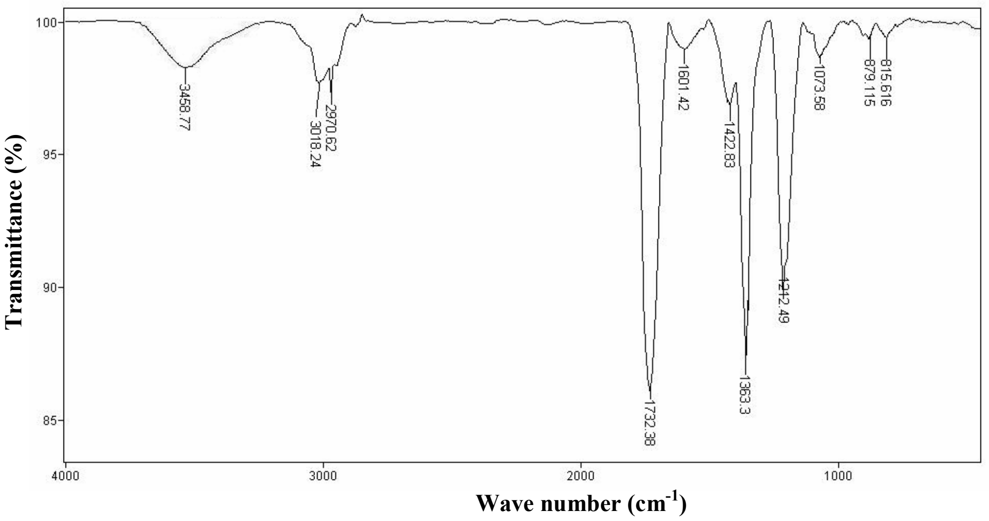

Figure 1: FTIR spectra of the precursor I.

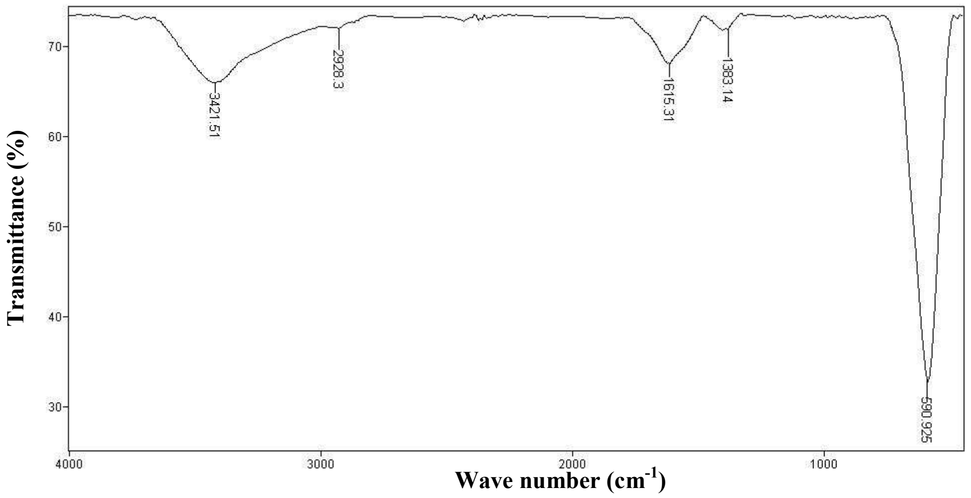

Figure 2: FTIR spectra of the precursor II.

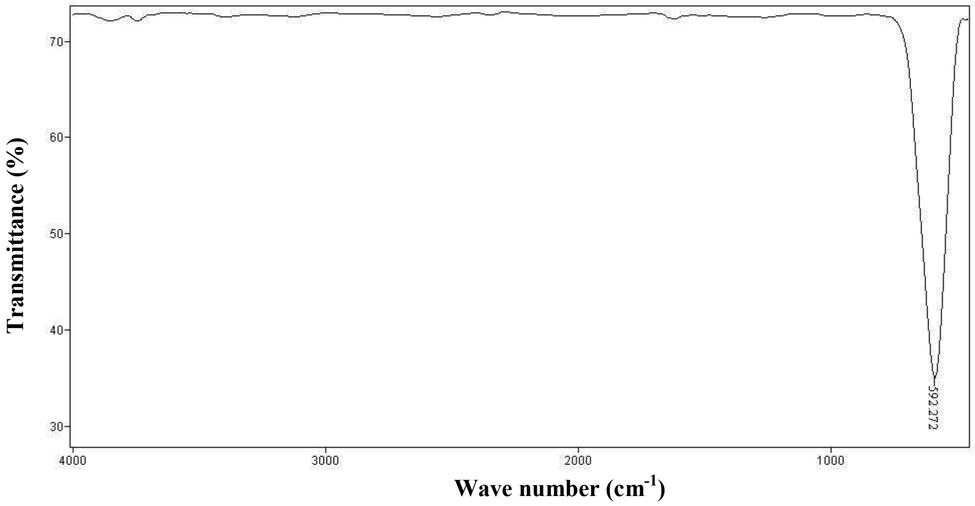

Figure 3: FTIR spectra of the cobalt ferrite powder.

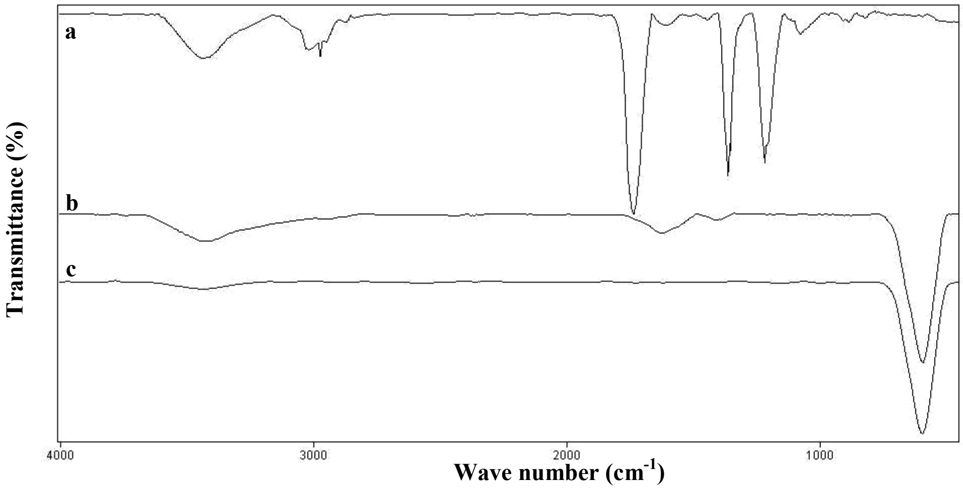

Figure 4: Comparison between FTIR spectra of the precursor I (a), precursor II (b) and cobalt ferrite powder (c).

Figure 5 shows the thermal analysis (TG-DTG-DTA) of the precursor I. In the thermal analysis, the physical property of a sample is measured as a function of temperature, while the sample is subjected to a controlled temperature program. Thermogravimetric analysis (T_G) is done on samples to determine changes occurred with rising temperature. In differential thermal analysis (DTA), the temperature difference which may develop between a sample and an inert reference material is measured, when both are subjected to simultaneous heating.

The obtained thermogravimetery (T_G) and derivative thermogravimetery (DTG) curves show three stages of weight loss. The total weight loss up to 400 °C is 90%, which is typical of synthesis processes using polymeric precursor routes. First one about 170 °C is related to the loss of water and some adsorbed gases on the surface. The second and third ones are ascribed to the decomposition of the organic matter with the consequent elimination of CO_2 from polymeric chains bound to the metallic ions to form oxides. The results confirmed by the evaluation of the derivative curve of the thermogravimeteric analysis (DTG), indicats a decomposition reaction of type II which is accompanied by exothermic peaks in the differential thermal analysis (DTA) curve [19]. It is suggested by the literature [20] that metal complexes prepared by this technique may present two main types of decomposition reactions. Type I is characteristic of a continuous weight loss, whereas type II is a stepwise reaction caused by the formation of an intermediate complex. The main difference between these decomposition reactions is the relative stability of the precursor. After 400 °C the weight loss is negligible.

The DTA curve exhibit a large exothermic peak starting at ~350 °C and extending up to ~400 °C which can be ascribed to the burn off organic materials. This may confirm that the majority of the mass loss occurs just below ~400 °C which allows optimization of heating program. These results are in agreement with the infrared spectroscopy.

Figure. 6 shows the XRD pattern of the sample after heat treatment at 500 °C for 2 hours. XRD patterns are based on observations of the scattered intensity of an incident X-ray beam on a powder sample as a function of the scattered angle and wavelength. The observations reveal information about the crystallographic structure and crystallite size of the sample. By comparing the obtained pattern with the relevant JCPDS (Joint Committee for Powder Diffraction Standards) patterns, the obtained XRD result has confirmed the formation of the pure single-phase cobalt ferrite with the cubic spinel structure and the Fd3m (2 2 7) space group which is in agreement with the FTIR results.

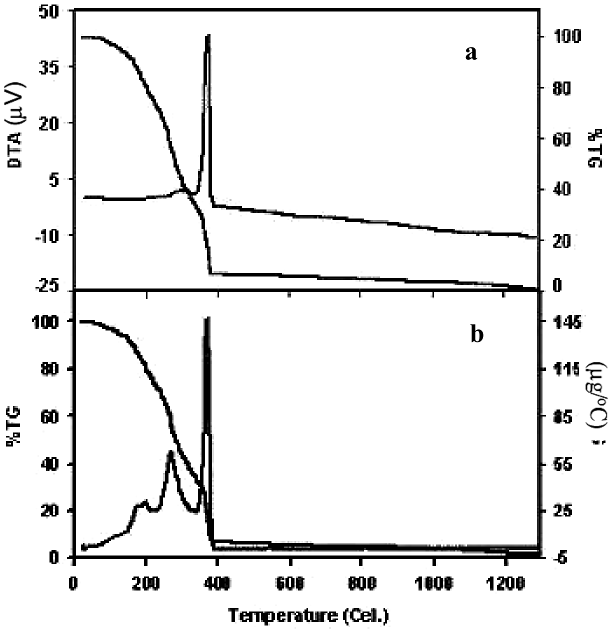

Figure 5: Thermal analysis of the precursor I, TG-DTA (a) and TG-DTG (b).

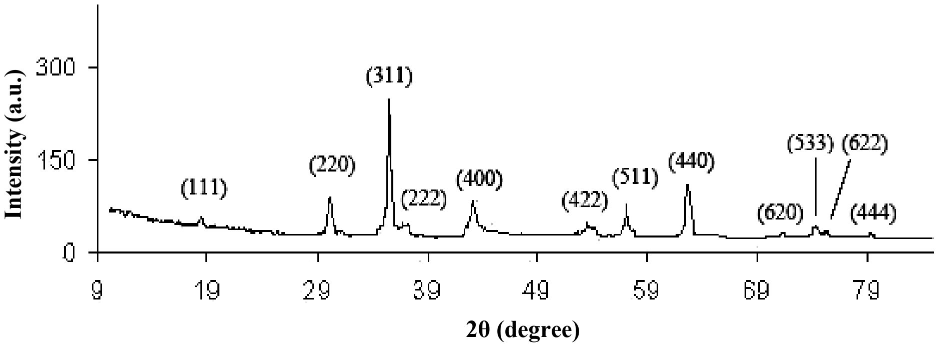

Figure 6: XRD pattern of the cobalt ferrite powder.

This material is usually synthesized by the solid state reaction, in which it is obtained after thermal treatment at 1100 or 1200 °C for more than 10 hours [21]. Therefore, the synthesis of cobalt ferrite via the coordinated precursor method leads to a significant decrease of the synthesis temperature. The determined lattice constant is 8.38 A which is in agreement with the typical value for the cobalt ferrite. The crystallite size is in the range of 18-22 nm as calculated by Scherrer equation (1) [22].

$$t = \frac{0.9\lambda}{\beta \cos\theta} \qquad (1)$$

where t is the crystallite size, λ the wavelength of X-ray radiation (Cu Kα), θ the Bragg angle and β is the full width at half maximum (FWHM) of the most intense diffraction peak (311) plane. According to the previous studies [3] substituting rare earth elements in the cobalt ferrite structure, causes the difficulties in the crystallization attributed to the relatively large ion radii of rare earth elements. More rare earth ions in B site of the spinel structure will result in both the higher necessary energy barrier for the crystallization as well as the more serious lattice distortion.

Scanning electron micrographs have been used to show the changes in the morphology of the precursors I, II and cobalt ferrite powder (Figures. 7 to 9).

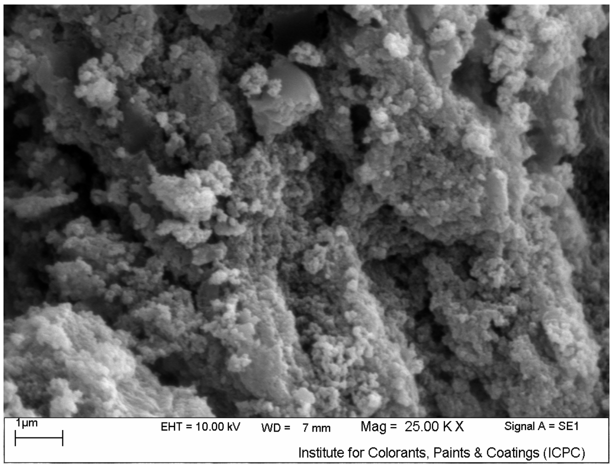

Figure 7: SEM micrograph of the precursor I.

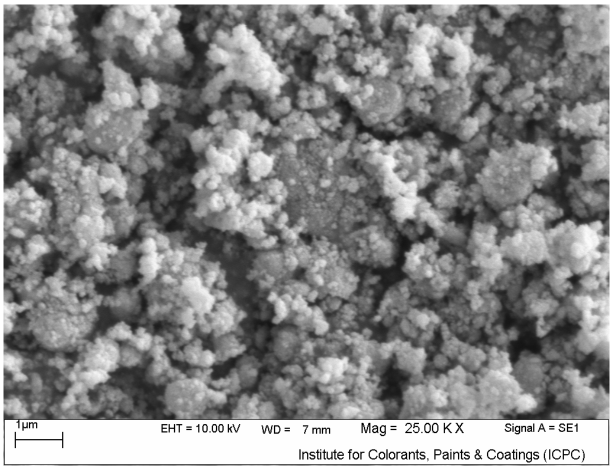

Figure 8: SEM micrograph of the precursor II.

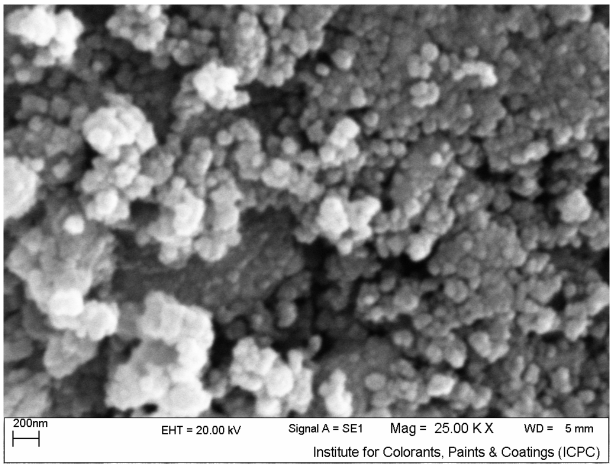

Figure 9: SEM micrograph of the cobalt ferrite powder.

The SEM micrograph of the cobalt ferrite powder (Figure 9) shows that the morphology of particles are almost spherical and regular in the shape, and are uniformly dispersed, whereas the precursors exhibit relatively porous networks. The scanning electron microscope images the sample surface by scanning it with a high energy beam of electrons in a raster scan pattern. The electrons interact with atoms of the sample and produce signals that contain information about the surface topography. By substituting rare earth elements in $CoFe_2O_4$, the formed powders may show different cubic and orthorhombic shapes due to the presence of the $CoFe_2O_4$ phase in cubic and $MFeO_3$ and M_2CoO_4 (M= rare earth element) phases in orthorhombic shapes [3]. The pressure exercised by gaseous species should be responsible for the break up of the porous structures.

The color of the cobalt ferrite pigment is evaluated from the $L^*a^*b^*$ colorimetric coordinates and diffuse reflectance spectroscopy. The CIE-$L^*a^*b^*$ colorimetric method as recommended by the Commission Internationale I´Eclairage (CIE) standards [23], has been used to measure the $L^*a^*b^*$ color parameters of the cobalt ferrite pigment. In this method, L^* varies from black (0) to white (100), b^* from blue (-) to yellow (+) and a^* from green (-) to red (+).Values of the colorimetric data L^*, a^* and b^* are found to be 18.039, 2.622 and 4.025, respectively. The values are less than obtained values for magnesium ferrite. The increase in the L^* parameter shows that sample provokes light dispersion and increases the brightness. Figure. 10 shows the color matched with the obtained $L^*a^*b^*$ color parameters in the Munsell Color System.

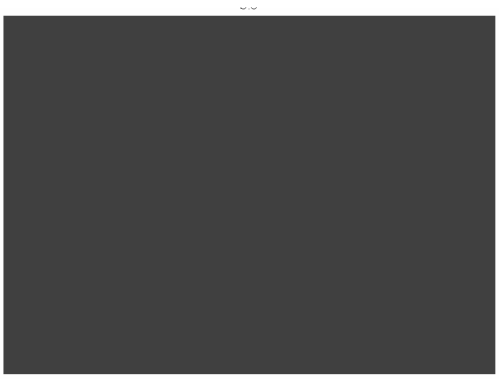

Figure 10: Color matched with the obtained L*a*b* color parameters in the Munsell Color System.

The diffuse reflectance spectrum of the cobalt ferrite pigment is shown in Figure 11. Results from the diffuse reflectance spectroscopy revealed nearly complete light absorption due to the very low intensity of the reflection in the 350-750 nm range. This has been further confirmed by the colorimetric coordinates. The relatively low values of L^*, a^* and b^* suggests full light absorption and confirmed the black color of the cobalt ferrite pigment which are in agreement with the color matched with the obtained $L^*a^*b^*$ color parameters in the Munsell Color System (Figure 10).

Figure 12 shows the hysteresis loop of the cobalt ferrite powder measured at room temperature which indicates the ferrimagnetic behavior. In the ferrimagnetic behavior, the octahedral and tetrahedral sublattice magnetizations are antiparallel and a noncompensated magnetic moment may occur. The sample has exhibited a hysteresis loop which is the typical of magnetic behavior. It indicates that the presence of an ordered magnetic structure can exist in the spinel system. Magnetic Coercivity (H_c) value measured for the sample is 1.8 kOe which shows the intensity of the applied magnetic field required for reducing the magnetization of the material to zero after the magnetization of the sample, has been driven to saturation. High Magnetic Coercivity (H_c) field may be due to the absence of moving of domain wells while being magnetized.

Values of the Saturation Magnetization (M_s) and Remanent Magnetization (M_r) are 67.72 emu/g and 32.54 emu/g, respectively. The M_s value measured for the sample is lower than the bulk value of 80 emu/g [24]. These results are in agreement with the previous studies which report the saturation magnetization value is 62.85 emu/g for the pure spinel cobalt ferrite samples having 21.5 nm diameters [3]. It is known that the energy of a magnetic particle in the external field is proportional to its particle size by the number of molecules in a single magnetic domain [25]. An increase in the particle size may lead to a decrease in the saturation magnetization due to the multidomain grains.

The lower saturation magnetization value associated with the nanocrystalline cobalt ferrite powder is being compared with the bulk which could be attributed to the structural distortions in the surface and the cation site occupancy in the nanosized cobalt ferrite. It is different from the bulk that gives the reduced magnetic moment [25].

The M_s value measured for the sample is more than the cobalt ferrite samples which have been substituted by rare earth elements. The magnetic moments in the case of rare earth element ions are generally originated from the localized 4f electrons. The net magnetic moments in the ferrite depend on the number of magnetic ions occupying the tetrahedral and octahedral sites. Therefore, the effect of rare earth element atoms in the cobalt ferrite materials seems to be similar to the substitution of non-magnetic atoms in the octahedral Fe sites of the spinel lattices, which reduces the M_s value.

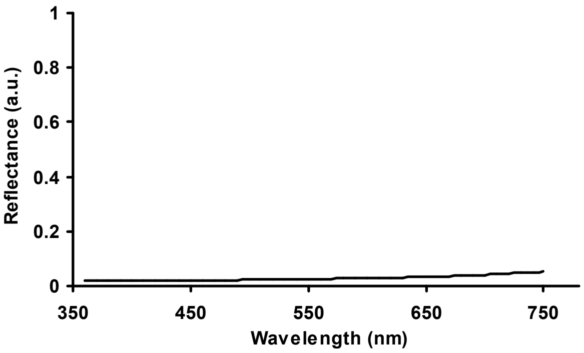

Figure 11: Diffuse reflectance spectrum of the cobalt ferrite pigment.

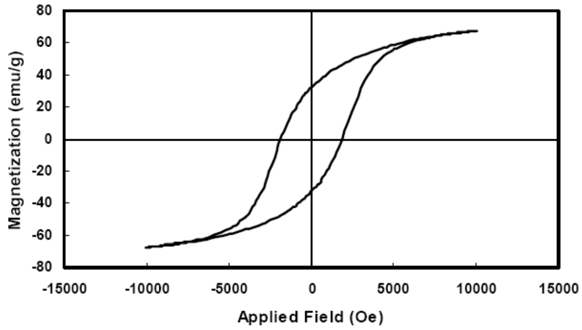

Figure 12: Hysteresis loop of the cobalt ferrite powder.

4. Conclusions

The coordinated precursors were used to synthesize magnetic nanocrystalline cobalt ferrite with a significant decrease of the synthesis temperature. The cobalt ferrite powder obtained presented the ferrimagnetic behavior and lower

the saturation magnetization value compared with the bulk. Our results indicated the formation of precursors with the coordination of carboxylate groups to the metal ions, in which metal ions were uniformly distributed throughout the organic matrix, lead to an important decrease of the synthesis temperature. The distribution of metal ions could greatly reduce the segregation of a particular metal during the processing which resulted into the preparation of very pure mixed oxides at low temperatures.

5. References

1. J. Popplewell, L. Sakhnini, The dependence of the physical and magnetic properties of magnetic fluids on particle size. *J. Magn. Mater.* 149(1995), 72-78.
2. C. V. Gopal Reddy, S. V. Manorama, V. J. Rao, Semiconducting gas sensor for chlorine based on inverse spinel nickel ferrite. *Sensor Actuat. B: Chem.* 55(1999), 90-95.
3. C. A. Oliveira, R. M. Lago, R. V. R. A. Rios, R. Augusti, P. P. Sousa, W. N. Mussel, J. D. Fabris, The effect of Mn substitution on the catalytic properties of ferrites. *Stud. Surf. Sci. Catal.* 130(2000), 3789-3794.
4. D. Zins, K. Nakatsuka, F. Gendron, M. Rivoire, Evidence of reentrant behavior in nanoparticles of ferrite in ferrofluids. *J. Magn. Mater.* 201(1999), 84-87.
5. E. H. Kim, H. S. Lee, B. K. Kwak, B. Kim, Synthesis of ferrofluid with magnetic nanoparticles by sonochemical method for MRI contrast agent. *J. Magn. Mater.* 289(2005), 328-330.
6. P. Poddar, J. Gass, D. J. Rebar, S. Srinath, H. Srikanth, S. A. Morrison, E. E. Carpenter, Magnetocaloric effect in ferrite nanoparticles. *J. Magn. Mater.* 307(2006), 227-231.
7. P. A. Lessing, Mixed cation oxide powders via polymeric precursors. *Am. Ceram. Soc. Bull.* 68(1989), 1002-1007.
8. G. Visalakshi, G. Venkataswaran, S. K. Kulshreshta, P.N. Moorthy, Compositional characteristics of magnetite synthesised from aqueous solutions at temperatures up to 523K. *Mater. Res. Bull.* 28(1993), 829-836.
9. K. M. Reddy, L. Satyanarayana, S. V. Manorama, R. D. K. Misra, A comparative study of the gas sensing behavior of nanostructured nickel ferrite synthesized by hydrothermal and reverse micelle techniques. *Mater. Res. Bull*. 39(2004), 1491-1498.
10. Z. H. Zhou, J. Wang, X. Liu, H. S. O. Chan, Synthesis of Fe_3O_4 nanoparticles from emulsions. *J. Mater. Chem.* 11(2001), 1704-1709.
11. Y. T. Qian, Y. Xie, C. He, J. Li, Z. Y. Chen, Hydrothermal preparation and characterization of ultrafine magnetite powders. *Mater. Res. Bull.* 29(1994), 953-957.
12. T. Hyeon, S. S. Lee, J. Park, Y. Chung, H.B. Na, Synthesis of Highly Crystalline and Monodisperse Maghemite Nanocrystallites without a Size-Selection Process. *J. Am. Chem. Soc.* 123(2001), 12798-12801.
13. F. C. D. Lemosa, D. M. A. Meloa, J.E.C. Silvab, Up-conversion luminescence in Er^{3+}/Yb^{3+} codoped $PbTiO_3$ perovskite. *Mater. Res. Bull.* 40(2005), 187-192.
14. D. M. Boghaei, M. Gharagozlou, Synthesis and characterization of novel water-soluble zinc (II) Schiff-base complexes derived from amino acids and salicylaldehyde-5-sulfonates. *J. Coord. Chem.* 60(2007), 339-346.
15. D. M. Boghaei, M. Gharagozlou, M. Sayadi, Synthesis, characterization, electrochemical studies and catecholase-like activity of dinuclear copper(II) complexes of a phenol-based compartmental ligand. *J. Coord. Chem.* 60(2007), 2283-2295.
16. D. M. Boghaei, M. Gharagozlou, Spectral characterization of novel ternary zinc(II) complexes containing 1,10-phenanthroline and Schiff bases derived from amino acids and salicylaldehyde-5-sulfonates. *Spectrochim. Acta A.* 67(2007), 944-949.
17. S. C. Zhang, G. L. Messing, W. Huebner, M. M. Coleman, Synthesis of yttrium barium copper fibers from an Organic Acid. *J. Mater. Res.* 5(1990), 1806-1812.
18. K. Nakamoto, Infrared and raman spectra of inorganic and coordination compounds. Wiley, New York (1986).
19. A. Kundu, S. Anand, H. C. Verma, A citrate process to synthesize nanocrystalline zinc ferrite from 7 to 23 nm crystallite size. *Powder Technol.* 132(2003), 131-136.
20. P. Courty, H. Ajot, C. Marcilly, B. Delmon, Oxides mixtes ou en solution solide sous forme tres divisee obtenus par decomposition thermique de precurseurs amorphes. *Powder Technol.* 7(1973), 21-38.
21. A. I. Turkin, V. A. Drebushchak, Synthesis and calorimetric investigation of stoichiometric Fe-spinels: $MgFe_2O_4$. *J. Cryst. Growth.* 265(2004), 165-167.
22. B. D. Cullity, Elements of X-ray diffraction. Addison-Wesley Publishing Company, Reading, MA, 9(1956), 259.
23. CIE, Recommendations of Uniform Color Spaces, Color Difference Equations, Phychometrics Color Terms. Supplement No. 2 of CIE Publ. no. 15 (E1-1.31) 1971, Bureau Central de la CIE, Paris, (1978).
24. R. Valenzuela. Magnetic ceramics. Cambridge University Press, Cambridge (1994).
25. M. Rajendran, R.C. Pullar, A. K. Bhattacharya, D. Das, S. N. Chintalapudi, C. K. Majumdar, Magnetic properties of nanocrystalline $CoFe_2O_4$ powders prepared at room temperature: variation with crystallite size. *J. Magn. Magn. Mater.* 232(2001), 71-83.